Inclusion compounds of binaphthol with volatile guests: structures, selectivity and kinetics of desolvation

Luigi R. Nassimbeni* and Hong Su

Department of Chemistry, University of Cape Town, Rondebosch 7701, South Africa. E-mail: xrayluig@science.uct.ac.za

Received (in London, UK) 25th January 2002, Accepted 18th April 2002
First published as an Advance Article on the web 28th June 2002

Binaphthol forms inclusion compounds with 1,4-dioxane, morpholine, dimethylsulfoxide, acetone and tetrahydrofuran. The host:guest ratios of some of these compounds depend on the crystallisation temperature. Competition experiments between pairs of selected guests reveal different kinds of selectivity. Desolvation kinetics for these compounds yield similar activation energies of approximately 80 kJ mol^{-1}.

Introduction

The complementarity of molecular shape defines the process of molecular recognition, and the strengths and directionality of the various intermolecular interactions are responsible for the stability of a given host–guest compound. In their account of the nature of supramolecular interactions, Steed and Atwood[1] discuss the full range of forces which impinge on a molecular assembly. They vary from the strong ion–ion interactions (~250 kJ mol^{-1}) to the weak van der Waals interactions (< 5 kJ mol^{-1}). Of these, the strong hydrogen bond is particularly important in the design and selectivity of the host molecules, and its properties have been extensively reviewed.[2–6] More recently, the importance of weak hydrogen bonds of the type X–H···A, where X and A have low electronegativity, have been recognised and their parameters reviewed.[7] Aromatic interactions are also important, their geometry is variable and may involve a large number of functional groups.[8]

The design of host compounds which exhibit selective enclathration must take account of all of these interactions. Guanidium organodisulfonates have been employed to separate isomeric mixtures of xylenes and dimethylnaphthalenes by selective inclusion.[9] These hosts have been extensively studied and form the basis of crystal engineering of a range of lamellar structures.[10–12] While the design, synthesis and structures of a large number of host molecules and their inclusion compounds have been studied, their physical properties, such as thermal stability, kinetics of enclathration and desolvation, and mode of selectivity, have received relatively little attention.

We now present the results of the structural analyses, thermal stability, desorption kinetics and guest selectivity of the host 2,2′-dihydroxy-1,1′-binaphthyl (binaphthol, BINAP) with 1,4-dioxane (DOX), morpholine (MOP), dimethylsulfoxide (DMSO), acetone (ACT) and tetrahydrofuran (THF). The atomic numbering schemes of the inclusion compounds are shown in Scheme 1.

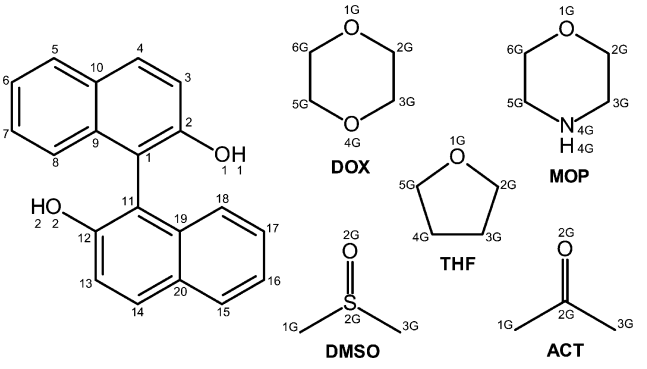

Scheme 1

Results and discussion

Crystal structure

Suitable single crystals of the inclusion compounds were obtained by dissolving the host in the liquid guests and allowing slow concentration over a period of 1–7 days. The temperature of crystallisation was carefully controlled as this can give rise to inclusion compounds of differing stoichiometries.[13,14] Thermogravimetry (TG) was employed to determine the host:guest ratios. Details of the crystal data, intensity data collections and refinement are given in Table 1. Cell dimensions were established from the intensity data measurements on a Nonius Kappa CCD diffractometer using graphite-monochromated Mo-Kα radiation. The strategy for the data collections was evaluated using the COLLECT[15] software. For all three structures, data were collected by the standard phi scan and omega scan techniques, and were scaled and reduced using DENZO-SMN[16] software. The structures were solved by direct methods using SHELX-86[17] and refined by full-matrix least-squares with SHELX-97,[18] refining on F^2. The program X-seed[19] was used as a graphical interface for structure solution and refinement using SHELX.

The refinement procedure for all structures was as follows: The positions of all the host atoms were obtained by direct methods and subsequent isotropic least-squares refinement yielded the positions of the guest atoms. All non-hydrogen atoms were refined anisotropically, except the tetrahydrofuran atoms in the BINAP·1.5THF structure. The hydroxyl hydrogens were located in difference electron density maps and refined with a simple bond length constraint which depended on a function of O–H *versus* O···O distances.[20] The remaining hydrogen atoms were placed in geometrically constrained positions and refined with isotropic temperature factors, generally

Table 1 Crystal data, data collection and final refinement parameters

Code of inclusion compound	BINAP·DMSO	BINAP·2DMSO	BINAP·1.5MOP	BINAP·ACT	BINAP·1.5THF
Guest	Dimethylsulfoxide	Dimethylsulfoxide	Morpholine	Acetone	Tetrahydrofuran
Host:guest ratio	1:1	1:2	1:1.5	1:1	1:1.5
Crystallisation temperature	25 °C/60 °C	4 °C	4 °C/25 °C	4 °C/25 °C/60 °C	4 °C/25 °C
Molecular formula	$C_{20}H_{14}O_2{\cdot}C_2H_6OS$	$C_{20}H_{14}O_2{\cdot}2C_2H_6OS$	$C_{20}H_{14}O_2{\cdot}1.5C_4H_9ON$	$C_{20}H_{14}O_2{\cdot}C_3H_6O$	$C_{20}H_{14}O_2{\cdot}1.5C_4H_8O$
Formula weight/g mol^{-1}	364.44	442.57	417.00	344.39	394.47
Crystal system	Monoclinic	Monoclinic	Monoclinic	Monoclinic	Orthorhombic
Space group	$P2_1/n$	$P2_1/c$	$P2_1/c$	$P2_1/n$	$Fdd2$
a/Å	20.792(3)	8.453(1)	9.139(2)	8.083(1)	14.651(2)
b/Å	8.883(1)	8.931(1)	27.672(6)	21.290(1)	55.471(6)
c/Å	20.800(3)	29.573(3)	9.204(2)	11.094(1)	10.259(1)
β/°	105.115(5)	92.928(1)	112.98(3)	107.36(1)	90
Volume/Å^3	3708.8(9)	2229.7(4)	2143.0(8)	1822.2(3)	8338(2)
Z	8	4	4	4	16
D_c/g cm^{-3}	1.305	1.318	1.292	1.255	1.257
μ/mm^{-1}	0.193	0.267	0.086	0.082	0.082
$F(000)$	1536	936	888	728	3360
Data collection temperature/K	293(2)	293(2)	173(2)	293(2)	173(2)
Range scanned θ/°	2.03–25.94	2.72–25.31	2.53–25.58	3.82–26.46	3.04–26.04
h, k, l ranges	−13–25, −9–10, −24–25	−10–6, −10–9, −35–33	0–10, −32–32, −11–9	0–10, −26–26, −13–13	−15–15, −58–33, −7–12
Measured, unique reflections	14062, 6074	5681, 3250	6543, 3760	5938, 3451	9863, 1537
Reflections observed [$I > 2\sigma(I)$]	4126	2652	1985	1973	1412
R_{int}	0.0472	0.036	0.0344	0.0346	0.0205
Data, restraints, parameters	6074, 8, 486	3241, 4, 308	3759, 5, 344	3541, 4, 247	1537, 5, 238
Final R indices [$I > 2\sigma(I)$], R_1	0.1197	0.0459	0.0919	0.0471	0.0993
wR_2 [$I > 2\sigma(I)$]	0.2698	0.1061	0.2147	0.1134	0.2664
Goodness of fit on F^2, S	1.160	1.051	1.050	0.980	1.032
Weighting scheme [where $P = (F_o^2 + 2F_c^2)/3$]	$w = 1/[\sigma^2(F_o^2) + (0.0322P)^2 + 40.288P]$	$w = 1/[\sigma^2(F_o^2) + (0.0325P)^2 + 1.584P]$	$w = 1/[\sigma^2(F_o^2) + (0.0951P)^2 + 2.150P]$	$w = 1/[\sigma^2(F_o^2) + (0.0646P)^2 + 0.00P]$	$w = 1/[\sigma^2(F_o^2) + (0.01868P)^2 + 74.31P]$
Extinction coefficient	0.0009(3)	0.005(3)	0.011(3)	0.042(6)	0.0028(8)
Max., min. $\Delta\rho$ in diff. e$^-$ density map/e Å^{-3}	0.976, −0.486	0.308, −0.241	0.472, −0.347	0.193, −0.130	0.824, −0.564

$1.2 \times U_{eq}$ of their parent atoms. All hydrogen bonds were located and their metrics are reported in Table 2.

CCDC reference numbers 184211–184215. See http://www.rsc.org/suppdata/nj/b2/b201255n/ for crystallographic data in CIF or other electronic format.

The structures of BINAP·1.5DOX and BINAP·3.5DOX have been reported previously.[13] However, we briefly describe their chief features because they are pertinent to the subsequent discussion of their kinetics of desolvation. In BINAP·1.5DOX each host molecule is hydrogen bonded to a

Table 2 Hydrogen-bonding details and torsion angle C(2)–C(1)–C(11)–C(12) (t_1) of host

Inclusion compound	Torsion angle t_1/°	D–H···A[a]	H···A/Å	D···A/Å	∠DHA/°
BINAP·DMSO	95.5(3)	O(1X)–H(1X)···O(1GA)[b]	1.76(2)	2.727(7)	168(7)
	100.3(9)	O(2X)–H(2X)···O(2GB)	1.73(2)	2.698(8)	171(8)
		O(1Y)–H(1Y)···O(2GA)	1.78(2)	2.720(8)	157(5)
		O(2Y)–H(2Y)···O(2GB)[c]	1.66(2)	2.662(8)	175(9)
BINAP·2DMSO	104.8(3)	O(1)–H(1)···O(2GA)[d]	1.72(1)	2.666(2)	176(3)
		O(2)–H(2)···O(2GB)[e]	1.68(1)	2.641(3)	168(3)
BINAP·1.5MOP	102.8(5)	O(1)–H(1)···O(1GA)	1.66(2)	2.586(9)	155(4)
		O(1)–H(1)···O(1A)	2.08(2)	3.06(1)	173(4)
		O(2)–H(2)···O(1GB)/N(4GB)	1.82(2)	2.762(4)	165(4)
BINAP·ACT	92.1(2)	O(1)–H(1)···O(2G)	1.99(1)	2.849(2)	147(2)
		O(2)–H(2)···O(2G)[f]	1.86(1)	2.807(2)	179(2)
BINAP·1.5THF	94.5(5)	O(1)–H(1)···O(1GA)[g]	1.66(2)	2.61(1)	161(6)
		O(2)–H(2)···O(1GB)[h]	2.17(2)	3.05(2)	152(6)

[a] Donor (D)–H···acceptor (A). Symmetry codes:[b] x, $y-1$, z. [c] $x+1/2$, $-y+1/2$, $z+1/2$. [d] $-x+1$, $y-1/2$, $-z+1/2$. [e] $-x+1$, $-y$, $-z$. [f] $-x+1$, $-y$, $-z+2$. [g] $x-1/4$, $-y+1/4$, $z-1/4$. [h] $x+1/2$, y, $z-1/2$.

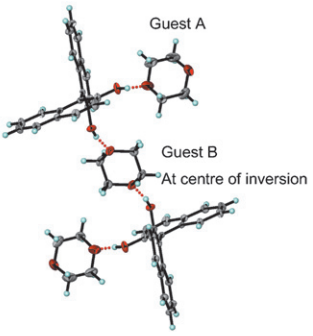

Fig. 1 Hydrogen bonding in BINAP·1.5DOX.

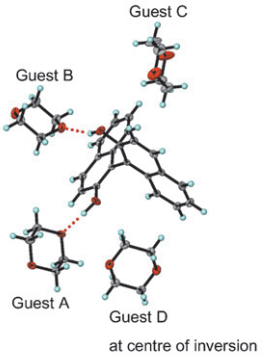

Fig. 2 Hydrogen bonding in BINAP·3.5DOX.

single dioxane (A), and a second dioxane (B), located on a centre of inversion, links two host molecules. Fig. 1 shows the cluster of two host and three guest molecules.

In BINAP·3.5DOX, the host is hydrogen bonded to dioxanes A and B, while dioxanes C and D (the latter located at $\bar{1}$) are only stabilised by van der Waals interactions. This is shown in Fig. 2.

BINAP·DMSO crystallised at 25 and 60 °C in the space group $P2_1/n$ with $Z = 8$. The asymmetric unit consists of two host and two guest molecules, all located in general positions. The DMSO guests act as hydrogen-bonding bridges between pairs of host molecules, giving rise to continuous ribbons of host–guest pairs running parallel to [101] (Fig. 3). The DMSO guests lie in centrosymmetric lacunae which accommodate pairs of guests.

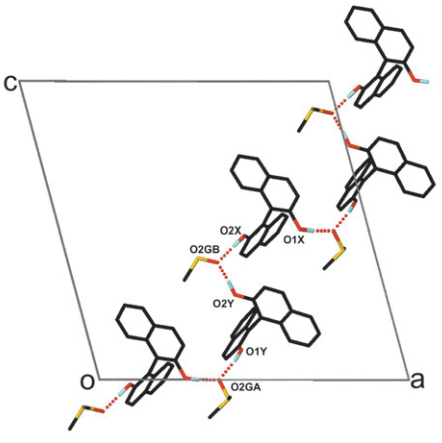

Fig. 3 Ribbon of host–guest pairs running in the [101] direction in BINAP·DMSO.

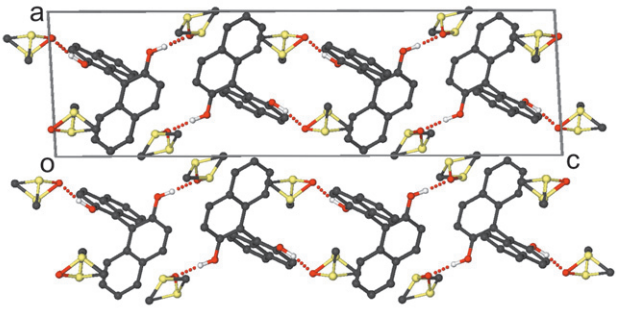

Fig. 4 Projection of BINAP·2DMSO viewed along [010].

BINAP·2DMSO crystallised at 4 °C in the space group $P2_1/c$ with $Z = 4$; all molecules are in general positions. Both DMSO guests were disordered, with S atoms occupying two positions. Their site occupancies refined to 0.73 and 0.27 (guest A), and to 0.62 and 0.38 (guest B). This is a common form of disorder for DMSO molecules in inclusion compounds.[21] The structure is tubulate, with the DMSO molecules lying in channels running parallel to [100] and [010] (Fig. 4). Each hydroxyl moiety of the host acts as a hydrogen-bond donor to a DMSO molecule.

BINAP·1.5MOP crystallised at 4 and 25 °C in the space group $P2_1/c$ with $Z = 4$. The cell dimensions are similar to those of BINAP·1.5DOX and the two structures may be regarded as isostructural with respect to the host positions. The morpholine located in the general position is, however, disordered and the molecule was placed on two sites, with site occupancies of 0.54 and 0.46, respectively. The second morpholine, located on a centre of inversion at Wyckoff position *c*, was refined with common positions for the O and N atoms, each with site occupancies of 0.5. The topologies of the two structures are similar, and they give rise to comparable powder diffraction patterns.

BINAP·ACT crystallised at 4, 25 and 60 °C in the space group $P2_1/n$ with $Z = 4$, all molecules being located in general positions. The acetone oxygen accepts two hydrogen bonds from adjacent host molecules, giving rise to a closed tetramer comprising two hosts and two guests, as shown in Fig. 5. The guests are located in channels running parallel to [101].

BINAP·1.5THF crystallised at 25 °C in the space group *Fdd*2 with $Z = 16$. The host and one THF guest were placed in general positions, and the remaining THF was located on a diad at Wyckoff position *a*. The BINAP is hydrogen bonded

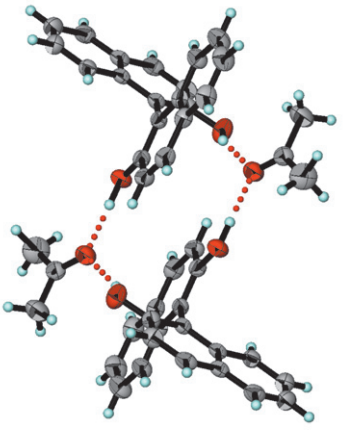

Fig. 5 Tetramer of two BINAP molecules and two acetones, linked by hydrogen bonds.

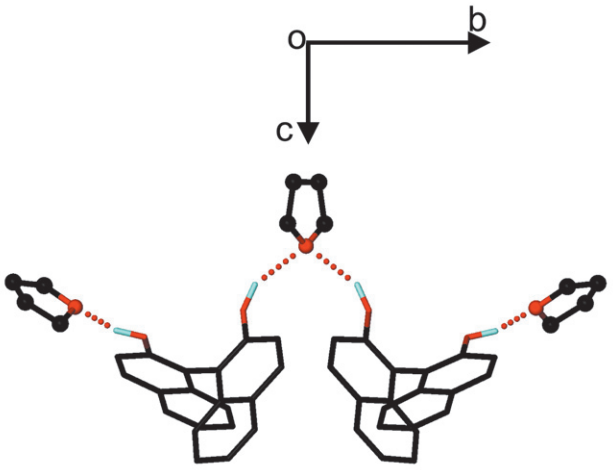

Fig. 6 Hydrogen bonding in BINAP·1.5THF.

to the THF in the general position, while the guest located at the diad acts as an acceptor to two symmetry-related hosts, as shown in Fig. 6. All guests are located in cavities created by the host molecules.

The torsion angles C(2)–C(1)–C(11)–C(12), which define the conformation of the hosts, are listed in Table 2. They vary from 92.1(2) to 104.8(3)°.

Selectivity

Competition experiments between two guests were carried out in solutions as follows. A series of 11 vials was made up with mixtures of two guests, such that the mole fraction of a given guest varied from 0 to 1. The host was added to each mixture, keeping the ratio of total guest to host at about 15:1 and dissolved by warming. The vials were left open at room temperature and the resulting crystalline inclusion compounds were filtered off, dried and dissolved in chloroform. These solutions, as well as the mother liquors, were analysed by gas chromatography.

In general, three kinds of selectivity curves arise, as shown in Fig. 7. X_A is the mole fraction of guest A in the liquid mixture and Z_A that of guest A which has been enclathrated in the host–guest crystal. The diagonal line represents zero selectivity. Curves b1 and b2 occur when guest A is strongly selected over guest B for the whole concentration range. Following Ward,[9] we may define a selectivity coefficient:

$$K_{A:B} = (K_{B:A})^{-1} = Z_A/Z_B \times X_B/X_A (X_A + X_B = 1)$$

Thus, $K_{A:B} = 1$ yields curve a, $K_{A:B} = 2$ and 8 yield curves b_1 and b_2, respectively, while curve c results when the selectivity is concentration dependent.

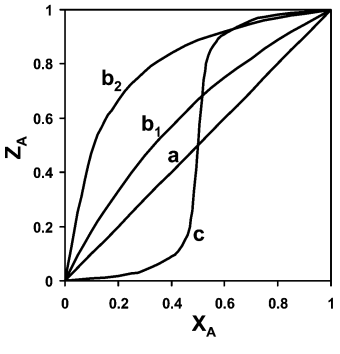

Fig. 7 General types of selectivity curves.

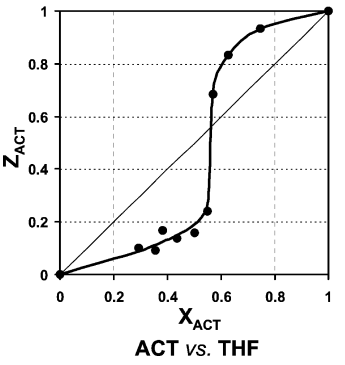

Fig. 9 Selectivity of acetone *versus* tetrahydrofuran, exhibiting concentration dependence.

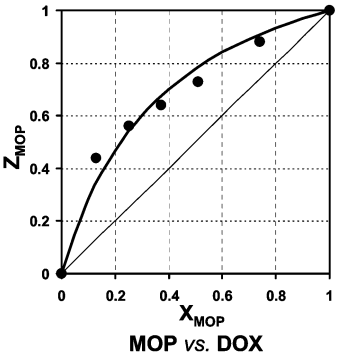

Fig. 8 Selectivity of morpholine *versus* 1,4-dioxane. The points lie close to a curve of $K = 3.5$.

We carried out competition experiments between morpholine and dioxane at 25 °C. The results are depicted in Fig. 8, which shows that morpholine is favoured by BINAP over the whole concentration range. The experimental points lie close to a selectivity coefficient of 3.5.

In contrast, the competition experiments carried out between acetone and tetrahydrofuran, Fig. 9, shows the results to be concentration dependent, acetone being enclathrated when its mole fraction is > 0.58, while THF is favoured below this limit. This phenomenon has been noted for binaphthol in the separation of 2,4- and 2,6-lutidine.[22] An important aspect of this kind of selectivity occurs in the separation of 3- and 4-picoline by bulky diol hosts.[23] In this study, it was shown that the sigmoidal selectivity curve changed position depending on the presence of neutral solvents, but no systematic work on this aspect has been carried out.

Thermal analysis

Thermogravimetry (TG) and differential scanning calorimetry (DSC) were carried out on a Perkin–Elmer PC7-Series system. The experiments were performed over a temperature range of 30–230 °C at a constant heating rate of 10 °C min^{-1}, with a purge of dry nitrogen flowing at 30 ml min^{-1}. The samples were crushed, blotted dry and placed in open platinum pans for TG experiments, and in crimped but vented aluminium pans for DSC. The results of the TG analyses are displayed in Fig. 10, and relevant thermal data are given in Table 3.

The TG trace shows that BINAP·DMSO desorbs in a single step [Fig. 10(a)], the corresponding endotherm showing an onset temperature of $T_{on} = 153$ °C, followed by a sharp endotherm corresponding to the host melt. BINAP·2DMSO desorbs in two distinct steps [Fig. 10(b)], each corresponding to the loss of a single DMSO guest, and DSC shows two concomitant endotherms, one broad ($T_{peak} = 123$ °C) and one

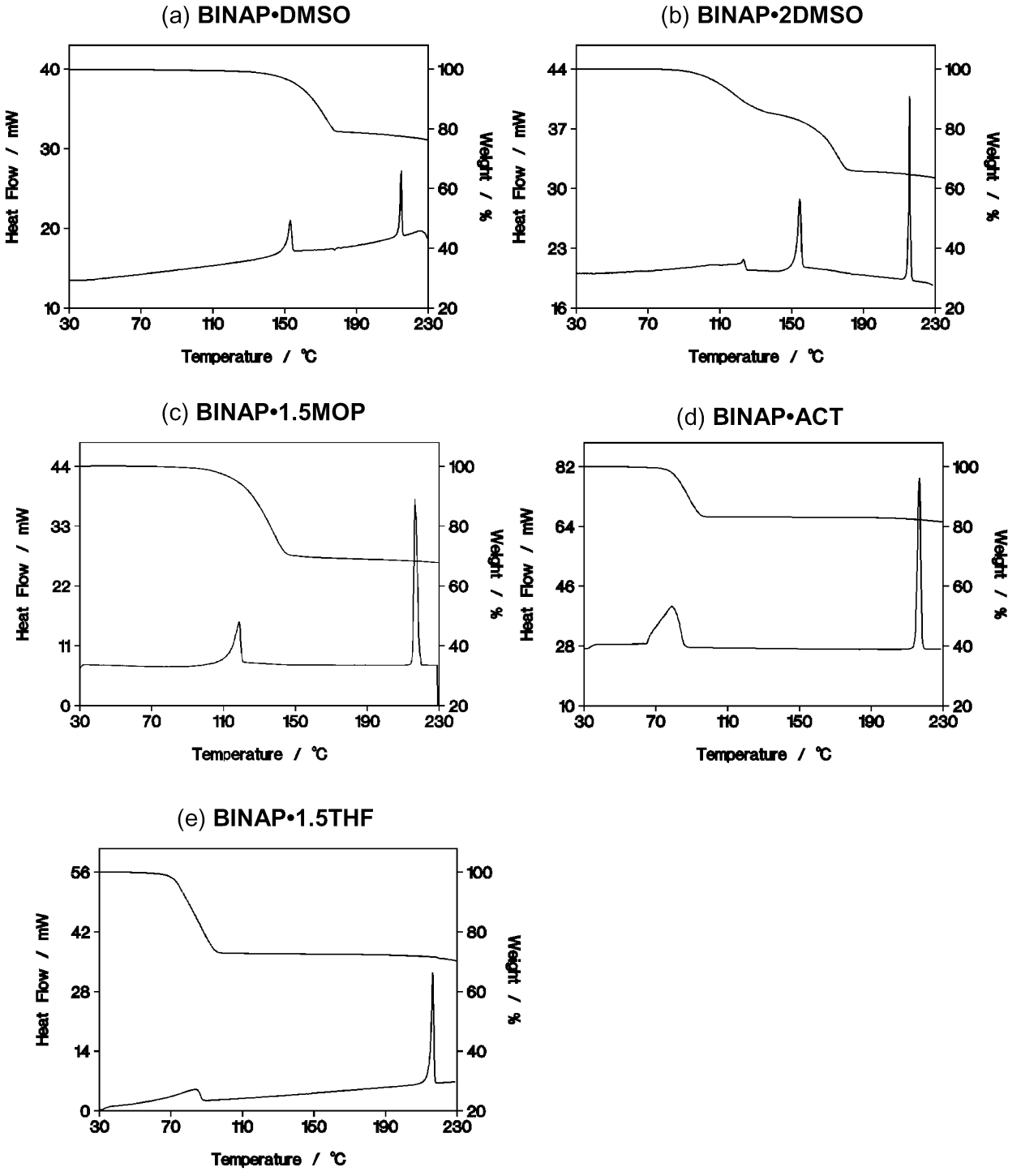

Fig. 10 TG and DSC curves for the inclusion compounds.

Table 3 Relevant thermal analysis data for the inclusion compounds

Inclusion compounds	Observed weight loss from TG (%)	Calculated weight loss (%)	Guest release T_{on}/°C
BINAP·DMSO	20.9	21.44	153
BINAP·2DMSO	1st step 15.9	17.65	121
	2nd step 18.9	17.66	153
BINAP·1.5MOP	30.5	31.34	108
BINAP·ACT	16.6	16.86	65
BINAP·1.5THF	27.3	27.42	74

sharp ($T_{on} = 153\,°C$), followed by the host melt. BINAP·1.5MOP [Fig. 10(c)], BINAP·ACT [Fig. 10(d)] and BINAP·1.5THF [Fig. 10(e)] behave in a similar manner, with the TG traces exhibiting single mass losses and DSC giving the corresponding endotherms of guest release, followed by the host melts.

Kinetics of desolvation

For each compound analysed, a series of mass loss *versus* time curves were obtained at fixed, selected temperatures. The fraction decomposed, α, was calculated from the mass loss using $\alpha = (m_0 - m_t)/(m_t - m_f)$, where m_0 is the initial mass, m_t is

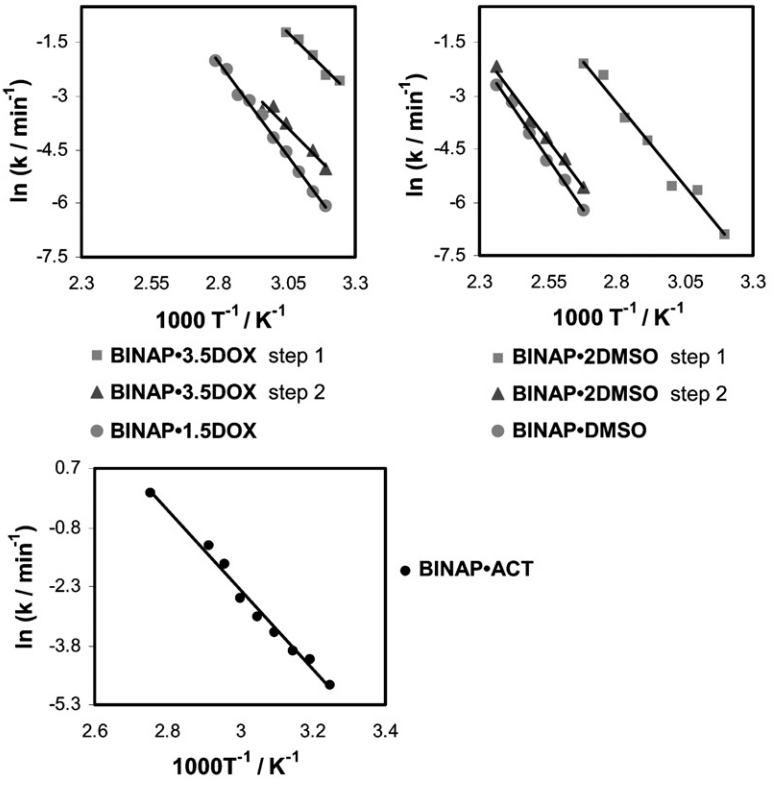

Fig. 11 Semilogarithmic plots of $\ln k$ *vs.* $1/T$ for desorption kinetics.

the mass at time t and m_f is the final mass. In the case of BINAP·3.5DOX and BINAP·2DMSO, both of which decompose in two distinct steps, each step was analysed separately using a temperature ramping technique.[24] The α–time curves were fitted to various models,[25] and judicious choice of the final equation took into account both the correlation factor and the α range over which the model fitted.[26] For the inclusion compounds containing dioxane and DMSO as guests, the desorption fitted the contracting area mechanism:

$$1 - (1 - \alpha)^{1/2} = kt$$

For BINAP·ACT, the α-time curves were sigmoidal and fitted the Avrami–Erofe'ev equation:

$$[-\ln(1 - \alpha)]^{1/2} = kt$$

The semilogarithmic plots of $\ln k$ *vs.* $1/T$ for each decomposition are shown in Fig. 11, and the relevant activation energies, together with other kinetic parameters, are given in Table 4. The activation energies are in the range 61 to 94 kJ mol^{-1}. Similar values were obtained for the desorption of acetonitrile from its inclusion complex with tenoxicam,[27] and for the desorption of benzene from its inclusion complex with the host *trans*-9,10-dihydroxy-di-*p*-*tert*-butylphenyl-9,10-dihydroanthracene.[28]

As discussed earlier, the decomposition of BINAP·3.5DOX occurs in two distinct steps:[13]

$$\text{BINAP} \cdot 3.5\text{DOX} \xrightarrow{-2\text{DOX}(T_{on}=45^{\circ}\text{C})} \text{BINAP} \cdot 1.5DOX \xrightarrow{-1.5DOX(T_{on}=85^{\circ}\text{C})} \text{BINAP}$$

The first step corresponds to the loss of two dioxane guest molecules. This is counterintuitive, only 2 of the 3.5 guest molecules are hydrogen bonded to the host and initial loss of only the 1.5 dioxane molecules which are not stabilised by hydrogen bonds would be expected. Indeed, this is what occurred in the desolvation of the inclusion compound 2,2′-bis(hydroxydiphenylmethyl)-1,1′-binaphthyl·3(pyridine), in which only one pyridine guest is hydrogen bonded to the host. This compound desorbs in two distinct steps, the first conforming to the loss of two pyridines ($T_{on} = 94\,^{\circ}$C), and the second to the loss of the remaining pyridine ($T_{on} = 143\,^{\circ}$C); it was surmised that the latter step corresponds to the hydrogen-bonded guest.[29]

The compound obtained after the first desorption step is identical to the BINAP·1.5DOX obtained from the crystallisation carried out at 60 °C. This was shown by matching the X-ray powder pattern of the compound obtained after the loss of 2 dioxanes with that calculated from the single crystal

Table 4 Kinetic parameters for the desolvation of inclusion compounds

Inclusion compound		Temp. Range/°C	α Range	Kinetic model	E_a/kJ mol^{-1}	In A
BINAP·3.5DOX	1st Step	35–55	0.05–0.90	R2	61(6)	21(2)
	2nd Step	40–65	0.10–0.90	R2	63(8)	19(3)
BINAP·1.5DOX		40–85	0.05–0.95	R2	86(2)	27(1)
BINAP·2DMSO	1st Step	40–100	0.05–0.95	R2	79(5)	23(2)
	2nd Step	100–150	0.10–0.90	R2	85(5)	22(1)
BINAP·DMSO		100–150	0.05–0.95	R2	94(3)	24(1)
BINAP·ACT		35–90	0.05–0.95	A2	85(4)	28(1)

structure of BINAP·1.5DOX. It is interesting to note that the activation energy obtained from the second step desorption of BINAP·3.5DOX is lower (63.8 kJ mol^{-1}) than that obtained from the freshly grown BINAP·1.5DOX, even though the compounds are identical. We attribute this to a particle size effect since we have noted that the crystallites obtained after the first desorption step are generally much smaller than those of the starting materials. The effect of crystallite size on decomposition kinetics is difficult to quantify,[30,31] but we have noted that at a given temperature, the rate of reaction increases with decreasing particle size. We note that the semilogarithmic plots for BINAP·3.5DOX (step 2) and BINAP·1.5DOX are very close, even though they yield somewhat different activation energies.

An analogous situation occurs in the desorption of BINAP·2DMSO, which occurs in two steps. The compound formed after the loss of one DMSO guest is identical to BINAP·DMSO synthesised from solution and the kinetic parameters follow a similar pattern to those of the dioxane inclusion compounds.

References

1 J. W. Steed and J. L. Atwood, *Supramolecular Chemsitry*, Wiley, Chichester, 2000, ch. 1.
2 G. A. Jeffrey, *An Introduction to Hydrogen Bonding*, Oxford University Press, Oxford, 1997.
3 G. R. Desiraju, *Crystal Engineering*, Elsevier, Amsterdam, 1989, ch. 5.
4 V. Bertolasi, P. Gilli, V. Ferretti and G. Gilli, *Acta Crystallogr., Sect. B*, 1995, **51**, 1004.
5 P. Gilli, V. Bertolasi, V. Ferretti and G. Gilli, *J. Am. Chem. Soc.*, 1994, **116**, 909.
6 M. C. Etter, *J. Phys. Chem.*, 1991, **95**, 4601.
7 G. R. Desiraju and T. Steiner, *The Weak Hydrogen Bond*, Oxford University Press, Oxford, 1999.
8 C. A. Hunter, K. R. Lawson, J. Perkins and C. J. Urch, *J. Chem. Soc., Perkin Trans. 2*, 2001, 651.
9 A. M. Pivotar, K. T. Holman and M. D. Ward, *Chem. Mater.*, 2001, **13**, 3018.
10 K. T. Holman, A. M. Pivotar, J. A. Swift and M. D. Ward, *Acc. Chem. Res.*, 2001, **34**, 107.
11 V. A. Russell, C. C. Evans, W. Li and M. D. Ward, *Science*, 1997, **276**, 575.
12 K. T. Holman and M. D. Ward, *Angew. Chem., Int. Ed.*, 2000, **39**, 1653.
13 L. R. Nassimbeni and H. Su, *J. Phys. Org. Chem.*, 2000, **13**, 368.
14 B. Ibragimov, *J. Inclusion Phenom. Macrocycl. Chem.*, 1999, **34**, 345.
15 COLLECT, Data Collection Software, Nonius, Delft, The Netherlands, 1998.
16 Z. Otwinowski and W. Minor, *Methods in Enzymology, Part A: Macromolecular Crystallography*, ed. C. W. Carter, Jr. and R. M. Sweet, Academic Press, 1997, vol. 276, p. 307.
17 G. M. Sheldrick, in *Crystallographic Computing*, ed. G. M. Sheldrick, C. Kruger and R. Goddard, Oxford University Press, Oxford, 1985, vol. 3, p. 175.
18 G. M. Sheldrick, SHELX-97, Program for Crystal Structure Determination, University of Göttingen, Germany, 1997.
19 L. J. Barbour, X-Seed, Graphical Interface for the SHELX Program, University of Missouri-Columbia, USA, 1999.
20 P. Schuster, G. Zundel and C. Sanderfy, *The Hydrogen Bond II, Structure and Spectroscopy*, North Holland Publishing Co., Amsterdam, 1976, 411.
21 L. J. Barbour, M. R. Caira and L. R. Nassimbeni, *J. Chem. Crystallogr.*, 1994, **24**, 539.
22 E. de Vries, L. R. Nassimbeni and H. Su, *Eur. J. Org. Chem.*, 2001, 1887.
23 K. Dohi, K. Tanaka and F. Toda, *J. Chem. Soc. Jpn., Chem. Ind. Chem.*, 1986, 927.
24 M. R. Caira, A. Coetzee, L. R. Nassimbeni, E. Weber and A. Wierig, *J. Chem. Soc., Perkin Trans. 2*, 1995, 281.
25 M. E. Brown, *Introduction to Thermal Analysis*, Chapman and Hall, London, 1988, ch. 13.
26 S. R. Byrn, R. R. Pfeiffer and J. G. Stowell, *Solid-State Chemistry of Drugs*, SSCI, West Lafayette, 2nd edn., 1999, ch. 21.
27 M. R. Caira, L. R. Nassimbeni and M. Timme, *J. Pharm. Sci.*, 1995, **84**, 884.
28 L. J. Barbour, M. R. Caira, A. Coetzee and L. R. Nassimbeni, *J. Chem. Soc., Perkin Trans. 2*, 1995, 1345.
29 E. Weber, K. Skobridis, A. Wierig, L. J. Barbour, M. R. Caira and L. R. Nassimbeni, *Chem. Ber.*, 1993, **126**, 1141.
30 M. E. Brown, *J. Therm. Anal.*, 1997, **49**, 17.
31 A. K. Galway and M. E. Brown, *Handbook of Thermal Analysis and Calorimetry*, Elsevier, Amsterdam, 1998, vol. 1, ch. 3.